AGU PUBLICATIONS

JGR

Journal of Geophysical Research: Atmospheres

RESEARCH ARTICLE
10.1002/2016JD025196

Key Points:
- New ground-based atmospheric ^{222}Rn monitoring stations in an underrepresented area of southwestern Europe
- First comparison of two portable atmospheric ^{222}Rn monitors: a single-filter progeny and a direct electrostatic deposition system
- Direct ^{222}Rn monitor response is not affected by rain and saturated atmospheric conditions

Supporting Information:
- Table S1
- Figure S1
- Supporting Information S1

Correspondence to:
C. Grossi,
claudia.grossi@ic3.cat

Citation:
Grossi, C., et al. (2016), Analysis of ground-based ^{222}Rn measurements over Spain: Filling the gap in southwestern Europe, *J. Geophys. Res. Atmos.*, *121*, 11,021–11,037, doi:10.1002/2016JD025196.

Received 6 APR 2016
Accepted 26 AUG 2016
Accepted article online 31 AUG 2016
Published online 17 SEP 2016

Analysis of ground-based ^{222}Rn measurements over Spain: Filling the gap in southwestern Europe

C. Grossi[1], A. Àgueda[1], F. R. Vogel[2], A. Vargas[3], M. Zimnoch[4], P. Wach[4], J. E. Martín[5], I. López-Coto[5,6], J. P. Bolívar[5], J. A. Morguí[1,7], and X. Rodó[1,8]

[1]Institut Català de Ciències del Clima (IC3), Barcelona, Spain, [2]Laboratoire des Sciences du Climat et l'Environnement, Paris, France, [3]Institut de Tècniques Energètiques, Universitat Politècnica de Catalunya, Barcelona, Spain, [4]Faculty of Physics and Applied Computer Science, AGH-University of Science and Technology, Krakow, Poland, [5]Departamento de Física, Universidad de Huelva, Huelva, Spain, [6]Now at National Institute of Standards and Technology, Gaithersburg, Maryland, USA, [7]Departament d'Ecologia, Universitat de Barcelona, Barcelona, Spain, [8]Institució Catalana de Recerca i Estudis Avançats, Barcelona, Spain

Abstract Harmonized atmospheric ^{222}Rn observations are required by the scientific community: these data have been lacking in southern Europe. We report on three recently established ground-based atmospheric ^{222}Rn monitoring stations in Spain. We characterize the variability of atmospheric ^{222}Rn concentrations at each of these stations in relation to source strengths, local, and regional atmospheric processes. For the study, measured atmospheric ^{222}Rn concentrations, estimated ^{222}Rn fluxes, and regional footprint analysis have been used. In addition, the atmospheric radon monitor operating at each station has been compared to a ^{222}Rn progeny monitor. Annual means of ^{222}Rn concentrations at Gredos (GIC3), Delta de l'Ebre (DEC3), and Huelva (UHU) stations were 17.3 ± 2.0 Bq m^{-3}, 5.8 ± 0.8 Bq m^{-3}, and 5.1 ± 0.7 Bq m^{-3}, respectively. The GIC3 station showed high ^{222}Rn concentration differences during the day and by seasons. The coastal station DEC3 presented background concentrations typical of the region, except when inland ^{222}Rn-rich air masses are transported into the deltaic area. The highest ^{222}Rn concentrations at UHU station were observed when local recirculation facilitates accumulation of ^{222}Rn from nearby source represented by phosphogypsum piles. Results of the comparison performed between monitors revealed that the performance of the direct radon monitor is not affected by meteorological conditions, whereas the ^{222}Rn progeny monitor seems to underestimate ^{222}Rn concentrations under saturated atmospheric conditions. Initial findings indicate that the monitor responses seem to be in agreement for unsaturated atmospheric conditions but a further long-term comparison study will be needed to confirm this result.

1. Introduction

Due to its physical characteristics, presented in classical literature such as *Fleischer et al.* [1980], *Tanner* [1980], *Nazaroff and Nero* [1988], *Nazaroff* [1992], and *Porstendorfer* [1994], the radioactive noble gas ^{222}Rn is widely used by the scientific community to study a number of different research topics, such as (i) to improve inverse transport models, which are used to calculate emissions of greenhouse gases (GHGs) [*Biraud et al.*, 2000; *Hirao et al.*, 2010; *Locatelli et al.*, 2015]; (ii) to study atmospheric transport and mixing processes within the planetary boundary layer [*Zahorowski et al.*, 2004; *Galmarini*, 2006; *Vinuesa et al.*, 2007; *Baskaran*, 2011; *Chambers et al.*, 2011, 2016; *Williams et al.*, 2011, 2013; *Grossi et al.*, 2012; *Vogel et al.*, 2013; *Hernández-Ceballos et al.*, 2015; *Vargas et al.*, 2015]; (iii) to improve radon flux inventories [*Szegvary et al.*, 2009; *Griffiths et al.*, 2010; *López-Coto et al.*, 2013; *Karstens et al.*, 2015]; (iv) to experimentally estimate GHGs fluxes by using the Radon Tracer Method [*Levin et al.*, 1999; *Vogel et al.*, 2012; *Wada et al.*, 2013; *Grossi et al.*, 2014]; (v) to understand the influence of climate change on the atmospheric radon increase and its associated health risks [*Nazaroff*, 2013; *Bochicchio et al.*, 2014; *Bossew et al.*, 2014]; and (vi) to refine baseline selection and characterization techniques and analyze air mass history and fetch at remote sites [*Zahorowski et al.*, 2004; *Chambers et al.*, 2013, 2014, 2015].

To deal with the above mentioned research issues, high-quality ^{222}Rn concentrations and flux observations are needed with high spatial resolution. Several worldwide monitoring networks of GHGs and air quality are already performing atmospheric ^{222}Rn gas measurements at different heights from the ground and using different measurement techniques [*Whittlestone and Zahorowski*, 1998; *Levin et al.*, 2002; *Zahorowski et al.*, 2005; *Xia et al.*, 2010; *Grossi et al.*, 2012; *Chambers et al.*, 2013, 2014, 2016]. Nevertheless, there is still a huge lack of data in southern Europe and, more generally, over the Mediterranean region. In addition, a

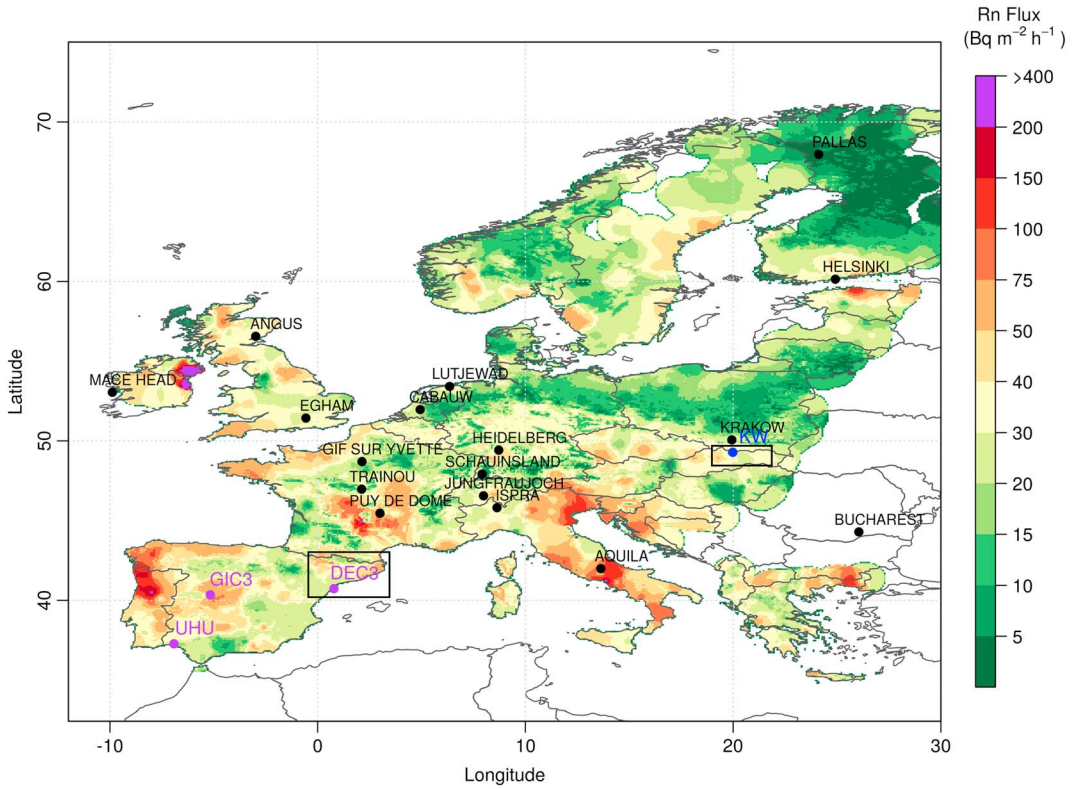

Figure 1. Location of operative atmospheric ^{222}Rn stations in Europe (black labels), recently established stations running in Spain (violet labels), and stations included in the ^{222}Rn monitors comparison exercise (black rectangles) overlaid on the 40 years retrospective climatology ^{222}Rn flux inventory by *López-Coto et al.* [2013].

harmonization of the experimental techniques applied for the measurements of atmospheric ^{222}Rn concentrations and ^{222}Rn fluxes is needed as suggested by the International Atomic Energy Agency [*International Atomic Energy Agency*, 2012]. European long-term ^{222}Rn monitoring stations, in agreement with the published literature, are presented in Figure 1 with black labels [e.g., *Chevillard et al.*, 2002; *Hatakka et al.*, 2003; *Taguchi et al.*, 2011; *Belviso et al.*, 2013; *Pitari et al.*, 2014; *Zimnoch et al.*, 2014; *Chambers et al.*, 2016], and the lack of stations over the Mediterranean Basin is noticeable.

To address this issue, the Institut Català de Ciències del Clima (IC3), in collaboration with the Institut de Tècniques Energètiques of the Universitat Politècnica de Catalunya (INTE-UPC) and the Universidad de Huelva (UHU), is deploying several atmospheric radon monitors (ARMONs) [*Grossi et al.*, 2012; *Vargas et al.*, 2015] in coastal and mountainous areas of Spain covering a broad range of regions with local radon flux source strengths ranging from 20 Bq m^{-2} h^{-1} to 180 Bq m^{-2} h^{-1} [*Szegvary et al.*, 2009; *López-Coto et al.*, 2013; *Karstens et al.*, 2015]. The ARMON is a recently improved electrostatic deposition system which has already been presented in details by *Grossi* [2012] and *Grossi et al.* [2012]. The main aim of this collaboration is to extend the monitoring of atmospheric ^{222}Rn concentrations carried out in Europe by other research institutes [e.g., *Levin et al.*, 2002; *Szegvary et al.*, 2009; *Belviso et al.*, 2013; *Zimnoch et al.*, 2014] offering high-quality data to the scientific community and working to fill the lack of harmonized ^{222}Rn data. Three stations: Gredos (GIC3), Delta de l'Ebre (DEC3), and Huelva (UHU), violet filled circles in Figure 1, are already operative and have been running continuously since December 2012, September 2013, and April 2014, respectively.

In the first part of the present study the performance of the ARMON detector was evaluated against that of a ^{222}Rn progeny monitor [e.g., *Levin et al.*, 2002] routinely operating in Krakow, Poland [*Zimnoch et al.*, 2014], under a range of high ambient temperature and relative humidity conditions. The short comparison exercise was conducted at two different stations: the Kasprowy Wierch mountain station located in Poland (Figure 1, KW blue label, black rectangle) and the Delta de l'Ebre coastal station situated in Catalonia, Spain (Figure 1, DEC3 violet label, black rectangle).

Table 1. Main Characteristics of the Spanish Atmospheric ^{222}Rn Stations Included in This Study

Station	Latitude; Longitude	Altitude (m asl)	Air Inlet (m agl)	Type of Station	Responsible Institution	Available Data Range	^{222}Rn Flux (Bq m^{-2} h^{-1}) [*López-Coto et al.*, 2013]
UHU	37.27°N; −6.92°W	10	10	City	UHU	4/2014 to 12/2015	30–40
DEC3	40.74°N; 0.79°E	0	10	Coastal	IC3	9/2013 to 12/2015	30–40
GIC3	40.22°N; −5.14°W	1440	20	Mountain	IC3	11/2012 to 12/2015	80–100

In the second part of this work, new observations from the three operative atmospheric ^{222}Rn stations, together with meteorological data, modeled ^{222}Rn fluxes, and regional footprint analyses have been used to (i) characterize the behavior of atmospheric ^{222}Rn concentrations under different seasonal and diurnal conditions at each station, (ii) understand the influence of local and/or regional atmospheric processes on the variability of atmospheric ^{222}Rn measured close to the ground at coastal and mountain areas, and (iii) qualitatively evaluate the influence of local versus remote radon sources.

2. Methodology

2.1. Atmospheric ^{222}Rn Monitoring Stations

2.1.1. Spanish ^{222}Rn Monitoring Stations

Atmospheric ^{222}Rn concentrations have been continuously measured at all three Spanish stations by ARMONs since mid-2014. Meteorological parameters (wind speed, wind direction, ambient temperature, relative humidity, and pressure) are also monitored at these stations at the same inlet heights (Table 1). In Figure 1 the locations of GIC3, DEC3, and UHU stations are presented (violet labels) overlapped with the averaged ^{222}Rn flux inventory calculated over 40 years of retrospective climatology by *López-Coto et al.* [2013].

The ARMON detectors were designed at the INTE-UPC laboratory and calibrated within a ^{222}Rn chamber under controlled environmental conditions [*Vargas et al.*, 2004; *Vargas and Ortega*, 2006]. Details of a typical ARMON calibration are reported in *Grossi* [2012] and *Grossi et al.* [2012].

In Table 1 a summary of the main characteristics of UHU, DEC3, and GIC3 stations is reported. Spanish stations are located at midlatitudes, between 35°N and 40°N, and covering a longitudinal interval between 7°W and 1°E.

UHU station started operating in April 2014. In addition to ^{222}Rn concentrations, atmospheric dry and wet deposition and PM10 are measured at this station. The station is located in Huelva city (around 150,000 inhabitants), about 10 km from the SW Atlantic coast of Spain (Gulf of Cádiz) and between two rivers (Tinto and Odiel). Huelva is on the most westerly vertex of the triangle that the Guadalquivir valley defines between Sierra Morena hills (400 km length; 800 m above sea level (asl) average height) and the Sistema Bético mountains (800 km length; 1200 m asl average height). On the eastern side of Huelva city, approximately 1–2 km from the station, there are several phosphogypsum (PG) piles covering an area of 12 km^2 [e.g., *Bolívar et al.*, 1996, 2002; *Hernández-Ceballos et al.*, 2015].

DEC3 is located on the eastern coast of Spain, within the Ebre River Delta (ERD), which is one of the largest wetland areas (over 300 km^2) in the northwestern Mediterranean region [*García et al.*, 1993], and it is flooded for most of the year (8–10 months). The ERD is a frontier region between the Mediterranean Sea and a region of rice fields. Strong winds coming from the north of Spain have been observed at this station [*Gangoiti et al.*, 2002]. DEC3 station is also influenced by sea breeze phenomena mainly during the summer [*Martín et al.*, 1991]. Atmospheric ^{222}Rn concentrations have been measured at DEC3 since September 2013 together with CH_4, CO_2, N_2O, and CO. DEC3 was one of the two stations where the comparison exercise between ARMON and a ^{222}Rn progeny monitor was carried out in summer 2011.

GIC3 is located in the Parque Regional de la Sierra de Gredos at the inner Iberian Plateau and 170 km SW of Madrid (3.1 million inhabitants). The mountains of Gredos feature the highest mountain range in the E-W orientated central mountain system that divides the Iberian Peninsula in two parts. Atmospheric ^{222}Rn concentrations have been measured at GIC3 since December 2012 together with atmospheric concentrations of CH_4 and CO_2 [*Grossi et al.*, 2014].

The area surrounding GIC3 station is mainly composed of granitic soils. The average radon flux obtained by *Szegvary et al.* [2009] and *López-Coto et al.* [2013] for this region is of 80–100 Bq m^2 h^{-1}, almost twice the

average radon flux over Europe [*Karstens et al*., 2015]. On the contrary, areas surrounding DEC3 and UHU stations are mainly composed of sandy soils and modeled ^{222}Rn flux values at these locations range between 30 and 40 Bq m^{-2} h^{-1} [*Szegvary et al*., 2009; *López-Coto et al*., 2013; *Karstens et al*., 2015].

2.1.2. Comparison of ^{222}Rn Monitoring Stations

The electrostatic deposition versus single-filter ^{222}Rn detector comparisons were carried out in summer 2011 at two contrasting environments: DEC3 and Kasprowy Wierch (KW). At each location the ARMON and ^{222}Rn progeny monitors were running simultaneously and sampled the same air over a 7–9 days period in order to observe different synoptic episodes.

The first comparison study was carried at a continental high-altitude site, at the Kasprowy Wierch station (49.29°N, 19.98°E; KW blue label in Figure 1, black rectangle) in July 2011. The KW station is located in the south of Poland, within the High Tatra Mountains. The meteorological observatory hosting the monitoring station is located on the top of a mountain at 1989 m asl. The climate of the KW area is typical of a continental mountainous location, with relatively large diurnal and seasonal variations of temperature, high precipitation rates, frequent changes of atmospheric pressure, and strong winds [*Chmura et al*., 2008]. During the field campaign at KW most of the time a foggy weather conditions and several episodes of rainfall were observed. The south of Poland is characterized by high-frequency extreme precipitation events [*Łupikasza*, 2010]. Particularly, Tatra Mountains record between 816 mm and 1721 mm of average annual precipitation and the annual number of days with precipitation $\geq$1.0 mm is between 114 and 188, representing the 30% and 50% of the year, respectively [*Niedźwiedź et al*., 2014]. The atmospheric ^{222}Rn concentrations are not routinely measured at the KW station, and both ^{222}Rn monitors were running there only during the comparison study.

The second comparison study was performed in August 2011 at the Spanish DEC3 station described in section 2.1.1.

2.2. Footprint Analysis

Due to variations in the meteorological conditions, air masses arriving at the stations can be affected by ^{222}Rn sources of different areas: local and remote. Local and regional footprints influencing ^{222}Rn concentrations measured at each station have been evaluated by analyzing both observational data and model results. Local and regional footprints have been analyzed on a seasonal basis grouped as December, January, and February as winter; March, April, and May as spring; June, July, and August as summer; and September, October, and November as autumn.

1. The local footprint at each site has been analyzed using the wind data measured at each station (windrose analysis) on seasonal and on diurnal bases.
2. The regional footprint analysis offers information about the synoptic atmospheric circulation and the influence of ^{222}Rn remote source regions on ^{222}Rn concentrations variability. The Hybrid Single-Particle Lagrangian Integrated Trajectory (HYSPLIT) model (version 4) [e.g., *Draxler and Hess*, 1998; *Stein et al*., 2015] was used to study the main long-range air masses transport patterns for each station during different seasons. HYSPLIT was run with meteorological data from the Global Data Assimilation System reanalysis archive maintained by the Air Resources Laboratory (ARL) available at http://ready.arl.noaa.gov/. A subset of this data is available from ARL in a format suitable for transport and dispersion calculations using HYSPLIT with 2.5° global latitude-longitude projection and a temporal resolution of 6 h. Kinematic 3-D back trajectories in time (72 h) were computed for a period of 4 years (2012–2015) twice per day (at 12:00 UTC and 00:00 UTC), in order to include in the analysis diurnal and nocturnal atmospheric dynamics, and at 500 m above ground level (agl) following *Jorba et al*. [2004] and *Izquierdo et al*. [2014]. The footprint analysis was performed to integrate the results on a seasonal basis.

Although the meteorological inputs used for the HYSPLIT model have a low resolution, this is enough to study the regional atmospheric circulation and to perform a qualitative analysis of the different source regions influencing the atmospheric ^{222}Rn concentrations measured at each station during different seasons [e.g., *Chambers et al*., 2011; *Zimnoch et al*., 2014; *Chambers et al*., 2016]. The time period specified for the back trajectories (72 h) is related to the distance between source regions and the starting point. Seventy-two hours was selected because this period is representative enough of the long-range transport in the Iberian Peninsula as seen by other authors [*Jorba et al*., 2004; *Baeza et al*., 2012; *Hernández-Ceballos et al*., 2013; *Izquierdo et al*., 2014].

2.3. Emission Model for Local ^{222}Rn Sources

The ^{222}Rn flux model developed by *López-Coto et al*. [2013] was run in the present work to evaluate the possible influence of local sources at each ^{222}Rn monitoring station. The model is based on the fundamental equation of ^{222}Rn transport in porous media, taking into account the dependency of the transport coefficient on temperature and moisture content of the soil. This model has been compared with another available ^{222}Rn flux model and experimental ^{222}Rn flux data over Europe by *Karstens et al*. [2015]. The aforementioned comparison has shown that the difference between the two models is about 5–40% for ^{222}Rn fluxes over the Iberian Peninsula and that it is related to the ^{222}Rn emanation factor assumed for typical soils, the soil moisture input, and the snow cover information used by each model. In addition, the standard deviation reported by *López-Coto et al*. [2013] and calculated over 40 years of retrospective climatology is of about 30%. ^{222}Rn fluxes have been calculated for this study using simulated soil temperature and humidity parameters obtained from the Weather Research and Forecasting (WRF) model at 27 km of horizontal resolution and 1 h of temporal resolution [*López-Coto et al*., 2013]. ^{222}Rn fluxes were calculated between 2011 and 2014 because WRF simulations were only available for this period. Then, the time series of 4 years of ^{222}Rn fluxes at each station have been used to perform a climatological analysis of radon flux variability under different seasons.

It is worth noting that available ^{222}Rn flux models and inventories [*Szegvary et al*., 2009; *Griffiths et al*., 2010; *López-Coto et al*., 2013; *Karstens et al*., 2015] do not yet take into account any artificial radon source such as PG piles. In fact, phosphogypsum, which is a waste product of the phosphoric acid production process, generally contains high activity concentrations of ^{238}U series elements [*Dueñas et al*., 2007]. The Huelva PG piles (12 km^2) were included by the European Union in the list of radiological surveillance areas [*Dueñas et al*., 2007] because of possible radioactive impact on the atmospheric and aquatic environment, and past studies have shown activity concentrations between 500 and 1500 Bq kg^{-1} for ^{238}U series radionuclides. These concentrations are 30–50 times higher than in typical unperturbed soils and sediments [*Bolívar*, 1995, 1996; *Dueñas et al*., 2007; *Grossi*, 2012; *López-Coto et al*., 2014]. Theoretical work and experimental studies on ^{222}Rn flux at the Huelva PG piles have established values ranging between 50 Bq m^{-2} h^{-1} and 750 Bq m^{-2} h^{-1} depending on soil humidity and porosity and meteorological conditions [*Dueñas et al*., 2007; *Grossi*, 2012; *López-Coto et al*., 2014]. These PG piles represent a huge artificial and localized radon source which is not yet included in any ^{222}Rn flux inventory and could strongly influence atmospheric ^{222}Rn concentrations measured in their proximity under specific environmental conditions [*Grossi et al*., 2012; *Hernández-Ceballos et al*., 2015].

2.4. Comparison of Direct and by Progeny ^{222}Rn Monitors

ARMON detector was compared against single-filter ^{222}Rn progeny monitor. The KW ^{222}Rn progeny device usually operates at Krakow, which is located 100 km north of KW station [*Zimnoch et al*., 2014]. This monitor (henceforth referred to as monitor A) was initially developed at the Institute of Environmental Physics of the University of Heidelberg, Germany [*Levin et al*., 2002], and it is based on the α spectrometry of the ^{222}Rn daughters attached to the atmospheric aerosols and collected on a static quartz glass filter [*Porstendorfer*, 1994]. This model of ^{222}Rn monitor has been used at several European ^{222}Rn stations since 2002 [*Levin et al*., 2002; *Weller et al*., 2014; *Zimnoch et al*., 2014]. The ^{222}Rn concentration is calculated assuming a constant disequilibrium factor (F_{eq}) between ^{222}Rn and ^{214}Po in the atmosphere. *Levin et al*. [2002] derived a F_{eq} for ^{214}Po/^{222}Rn of 0.704 ± 0.081 for various meteorological conditions through parallel ^{222}Rn gas measurements with a slow pulse ionization chamber. This F_{eq} value was also used for monitor A in the comparison exercise. Monitor A, as reported by *Levin et al*. [2002], is suitable to measure hourly ^{222}Rn concentrations down to 500 mBq m^{-3} with an uncertainty well below ±20%.

The ARMON (henceforth referred to as monitor B) was developed at the INTE-UPC in 2008 [*Grossi*, 2012; *Grossi et al*., 2012; *Vargas et al*., 2015] and consists of two main modules: a detection volume (20 L) and an acquisition system for α spectrum analysis. The ARMON performs a direct measurement of ^{222}Rn and ^{220}Rn (thoron) concentrations based on the α spectrometry of ^{218}Po and ^{216}Po, respectively, on an implanted planar silicon detector surface and using a high electrostatic field. Sample air is first filtered to remove ambient aerosols and progeny, and new progeny is able to form as the sampled air mixes within, and passes through, the 20 L detector volume. The positive ions of polonium that are moved to the detector by the electrostatic field result exclusively from the α decay of ^{222}Rn and ^{220}Rn within the spherical detection volume. Monitor B

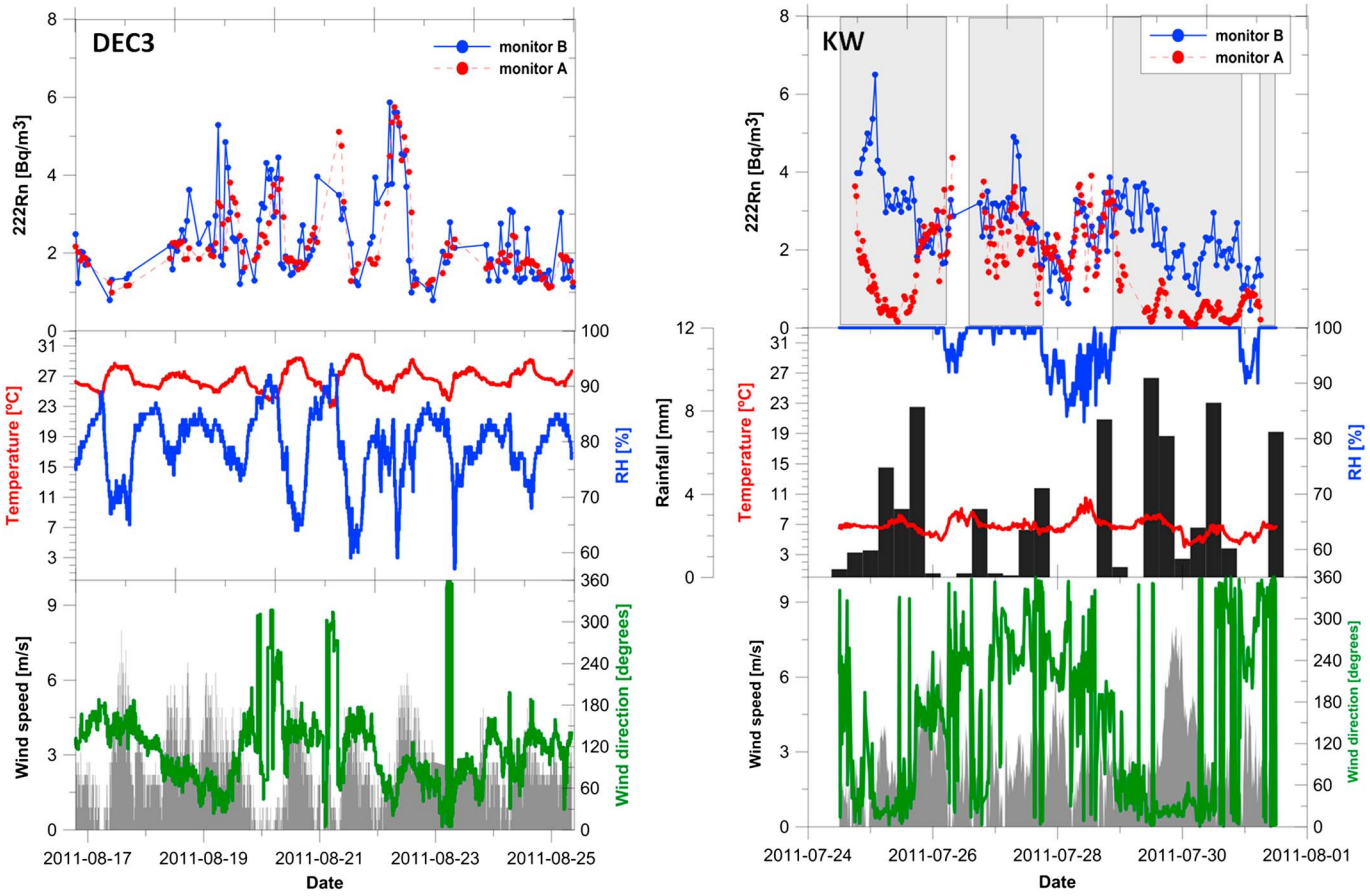

Figure 2. Hourly ^{222}Rn concentrations from monitors A and B and 10 min means of meteorological data (temperature, relative humidity (RH), wind speed, and wind direction) measured at the stations during both campaigns. (left column) DEC3 campaign and (right column) KW campaign. The 6-hourly accumulated rainfall data at KW station were obtained from Reliable Prognosis website (http://rp5.md/Weather_archive_in_Kasprowy_Wierch). Grey rectangles included in the ^{222}Rn data series from KW campaign highlight periods of water saturation (100% RH).

performs hourly measurements of atmospheric ^{222}Rn concentrations with a minimum detectable concentration of around 250 mBq m^{-3} [*Grossi*, 2012; *Vargas et al*., 2015].

3. Results and Discussion

3.1. ^{222}Rn Monitors Comparison

Atmospheric ^{222}Rn records and meteorological data obtained during the two comparison campaigns that took place during summer 2011 at DEC3 and KW stations are presented in Figure 2. During the comparison campaigns the measured ^{222}Rn concentrations were ranging between 0.6 ± 0.1 Bq m^{-3} and 6.3 ± 1.3 Bq m^{-3}. Although both comparison studies were not large enough for offering sufficient data to allow a robust statistical analysis and to properly constrain the relation between the responses of these two detectors, obtained results offer interesting insights to qualitatively evaluate the response of ARMON monitor under unsaturated and saturated atmospheric conditions. However, Figure S1 in the supporting information shows the observed correlations between both monitors obtained at DEC3 and KW stations during the short comparison campaigns.

^{222}Rn levels observed by both monitors during the days of parallel measurements at DEC3 station (Figure 2, left column) seem to agree. The mean value and its standard error, obtained at DEC3 station with the radon progeny monitor A is 2.25 ± 0.09 Bq m^{-3}, compared to 2.29 ± 0.10 Bq m^{-3} obtained with the radon gas monitor B. During the comparison campaign carried out at DEC3 station, the average ambient temperature was about 29°C and the relative humidity was always $<$100%. For situations with low ^{222}Rn air masses arriving at this coastal station, monitor B and monitor A agreed on minimal observed ^{222}Rn concentration, e.g., 0.80 ± 0.20 Bq m^{-3} and 0.99 ± 0.20 Bq m^{-3}, respectively, on 23 August.

During the comparison campaign at DEC3 (Figure 2, left column), ^{222}Rn concentrations measured by the monitor B show fast increases that were not observed by the monitor A. On this regard, *Levin et al*. [2016] reported a loss of ^{222}Rn progeny within the inlet tube due to the deposition of the aerosol on the internal walls of the tube. This artifact could lead to an underestimation of ^{222}Rn concentrations measured by the monitor A. In addition, this loss increases exponentially with the length of the sampling tube and the uncertainty of this correction is strongly increasing with the decrease of the atmospheric activity concentration [*Levin et al*., 2016]. This effect can obviously vary with the sampling site because it depends on the length of the inlet tube, the geometry of the inlet line, and the sampling flow, respectively. The estimation of the magnitude of this artifact is not included in the aim of the present study which focuses on the response of the ARMON.

At KW station monitor A showed, for 100% relative humidity (RH) and rainfall episodes with precipitation $\geq$ 1.0 mm, a significant reduction of the measured ^{222}Rn concentrations (Figure 2, right column). One or both of these conditions were fulfilled over 70% of the available data set. For the remaining 30% of the data set the agreement of both monitors at KW was comparable to that obtained at DEC3: measured mean ^{222}Rn concentrations by monitor A and monitor B were 2.26 ± 0.12 Bq m^{-3} and 2.13 ± 0.12 Bq m^{-3}, respectively.

These previous results are in agreement with results observed by *Xia et al*. [2010] which compared an one-filter ^{222}Rn progeny instrument (same type than monitor A) with a two-filter ^{222}Rn progeny monitor [e.g., *Zahorowski et al*., 2004] in a sampling site located in the Black Forest of southwest Germany, during 6 months. They found a good correlation between both monitors except for rainfall episodes. No evidence has been found in the literature of comparisons performed between ^{222}Rn progeny monitors and direct ^{222}Rn monitor, based on electrostatic deposition technique, such as the monitor B.

Thanks to the comparison with monitor B, it is also possible to observe that monitor A rapidly recovered when the relative humidity descended below 100% providing correct ^{222}Rn concentration measurements (e.g., see in Figure 2 the behavior of both KW ^{222}Rn data series during the night of 30 and 31 July 2011). The variability of the recovering time for part of the monitor A is not within the scope of this paper, and it should be further investigated in future and long-term comparison campaigns.

^{222}Rn progenies are very reactive elements, and thus, they get attached to aerosols quickly after they are produced in the air [*Porstendorfer*, 1994; *Baskaran*, 2011]. In a past study from *Porstendorfer et al*. [2000] it was observed that the size distribution of the aerosols, (to which ^{222}Rn progenies are usually found to be attached), can be approximated by the sum of three modes of a lognormal distributions which are differently effected by weather conditions. In addition, *Fujinami* [1996] explained how precipitation containing ^{222}Rn daughters mainly originates from scavenging within the cloud (rainout) and not from that below the cloud (washout). Finally, *Horng and Jiang* [2004] found an exponential decay relationship between ^{222}Rn progeny concentration in raindrops and rainfall rate.

These previous studies indicate that the underestimation of the ^{222}Rn concentrations measured by monitor A during KW campaign is probably due to a changing F_{eq} between ^{222}Rn and its ^{214}Po progeny in the sampled atmospheric air associated with variations in the humid deposition of aerosols with attached ^{222}Rn progeny.

To our knowledge no comprehensive investigation has been carried out yet to fully understand how the type of rain, its origin, its duration, and its rate affect the variability of the F_{eq} in outdoor air. In addition, the KW station is located at about 2000 m asl where the precipitation is usually formed. Thus, the characteristics of F_{eq} in rain at KW may be quite different from those observed at typical stations located at 0–200 m agl. The scope of the present study precludes a detailed investigation of these relationships, as it is mainly focused on the performance of ARMON. In addition, the available precipitation data for the monitor comparison at the KW station have a low temporal resolution of only 6 h accumulated totals. However, results presented in Figure 3 can give first important indications of the relationship between accumulated rainfall and F_{eq} variations. Actually, Figure 3 helps to better understand the variability of the ratio between the atmospheric ^{222}Rn concentration measured by monitor A (calculated with the constant disequilibrium factor declared by the manufacturer) and monitor B ($R_{A/B}$) in relation to the intensity of the rainfall events detected at KW station during the instrument comparison. An exponential decrease of $R_{A/B}$ is apparent with increasing accumulated rain, suggesting that the nominal disequilibrium factor between ^{222}Rn and its decay products could decrease by up to 80% during intense rain events at KW.

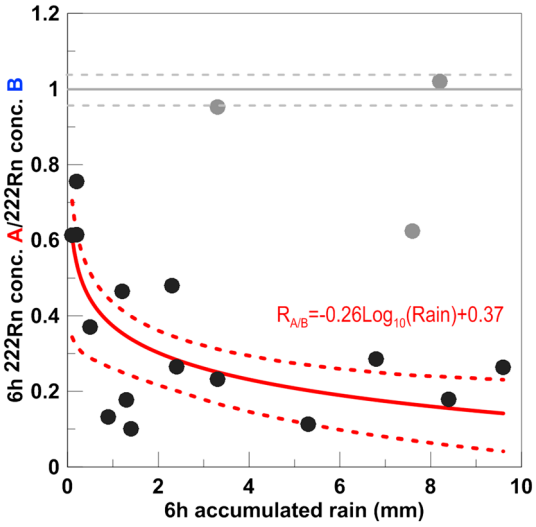

Figure 3. Ratio of 6-hourly mean values of atmospheric ^{222}Rn concentrations measured by monitor A to monitor B ($R_{A/B}$) in relation with 6-hourly total accumulated precipitation (mm) at KW station during the comparison exercise in summer 2011. Black circles: data observed under RH = 100%. Red line: regression line (continuous) obtained for black data points and 95% confidence interval lines (discontinuous) without considering the two points with $R_{A/B} \sim 1$ and the point with $R_{A/B} \sim 0.62$ with high accumulated rain (gray points). Grey lines: slope of the correlation line (continuous) and 95% confidence interval lines (discontinuous) obtained between both monitors at KW under the hypothesis of offset equal to 0.

Figure 3 also shows three episodes where $R_{A/B}$ does not follow in the observed empirical relationship. For two of those events the ratio of observed ^{222}Rn concentrations remains constant at the previous slope found at KW station under water unsaturated conditions (Figure 2, right column). The first of these previous events was observed on 25 July 2011 between 12:00 and 18:00 UTC. Figure 2 shows an increase in the wind speed at KW with winds changing from northerly to south-easterly. During this 6 h interval a recovery of ^{222}Rn concentration measured by the monitor A is observed. The second case was observed on 26 July 2011 again between 12:00 and 18:00 UTC. In this period wind direction changes largely between SW and north and wind speed was about 3 m s^{-1}. Finally, a third event was observed on 28 July 2011 again between 12:00–18:00 UTC. Here the observed $R_{A/B} = 0.62$ for high accumulated rain of 7 mm. The wind direction also in this episode varies between SW and north. All three of these previous cases can be explained with reference to the studies carried out by *Jagielski et al.* [1996] and *Spurny* [1999], who observed aerosol particles transported to the KW station from the valleys of the Tatra Mountain during diurnal valley-mountain breezes. Indeed, fresh aerosol arriving at the station from the valley could be attached to ^{222}Rn progeny producing an increase in the F_{eq} used by the monitor A and leading to a new increase of the ^{222}Rn concentrations measured by this monitor despite the rainfall.

Summarizing, although data in Figure 3 are not statistically significant to confirm the observed relationship, this result is quite interesting and it represents an important starting point to be further investigated in future analyses and long-term experiments.

3.2. Spanish ^{222}Rn Monitoring Stations

In the present section we perform a characterization of the behavior of atmospheric ^{222}Rn measured at the three Spanish operative atmospheric ^{222}Rn stations.

3.2.1. Modeled ^{222}Rn Fluxes

In Table 2 the seasonal ^{222}Rn flux means of 2011–2014 calculated from hourly estimated ^{222}Rn fluxes data set are reported for each station. This climatology offers useful information to understand measured atmospheric ^{222}Rn concentrations at each station during the different periods of the year.

Table 2. Seasonal ^{222}Rn Flux (Bq m^{-2} h^{-1}) Means (Mean Value ± Standard Deviation) at UHU, DEC3, and GIC3 Stations Obtained With the Model Developed by *López-Coto et al.* [2013] for the Period 2011–2014

	Season			
Station	Spring	Summer	Autumn	Winter
UHU	19 ± 6	36 ± 11	24 ± 7	17 ± 5
DEC3	30 ± 9	34 ± 10	34 ± 10	31 ± 93
GIC3	89 ± 27	140 ± 42	106 ± 32	73 ± 22

GIC3 and UHU stations display significantly higher values of ^{222}Rn fluxes in summer than during other seasons. This is due to dry soil ambient conditions registered during summer that facilitates the development of a vertical ^{222}Rn concentration gradient between the soil and the free atmosphere calculated by the ^{222}Rn flux model.

The model reflects the positive correlation between ^{222}Rn exhalation from the soil and ambient air temperature and a negative correlation with high soil moisture observed in past studies [*Nazaroff and Nero*, 1988; *Morawska*, 1989; *De Martino and Sabbarese*, 1997; *Grossi et al*., 2011; *Kamra*, 2015]. In the GIC3 area there is a significant difference between the calculated high summer ^{222}Rn fluxes, which have an average value of 140 Bq m^{-2} h^{-1} for the reported years, and winter fluxes, which are typically 50% lower (Table 2) due to the winter snow layer, present at these altitudes, which can prevent the ^{222}Rn exhalation form the soil [e.g., *López-Coto et al*., 2013].

In the UHU area the average ^{222}Rn flux ranges between 17 and 36 Bq m^{-2} h^{-1} for winter and summer, respectively. ^{222}Rn flux values calculated in the area of DEC3 station do not show a significant difference over the seasons (30–34 Bq m^{-2} h^{-1}). UHU and DEC3 areas are mainly characterized by sandy soil. Sand presents low ^{222}Rn concentrations which lead to low ^{222}Rn exhalation rates [*Rafique et al*., 2011; *Grossi et al*., 2012].

3.2.2. Footprints Results

3.2.2.1. Local Influence

Windrose plots from each station are presented in Figure 4 split by season and daytime/nighttime.

Windrose plots from UHU station show a high occurrence of northern winds for all the seasons with velocities up to 5 m s^{-1}. These winds seem to be particularly weak during the autumn. Northern winds are also more frequent at nighttime. They could be due to nocturnal flows coming from the Sierra Morena mountain, at the north of Huelva, and breeze phenomena occurring over this area during the night as observed by *Hernández-Ceballos et al*. [2015]. In contrast, daytime summer and spring windrose plots reflect the arrival of strong winds at the station, with velocities up to 10 m s^{-1}, coming from the southwest in direction of the Atlantic Ocean, as previously observed at the close El Arenosillo station by *Grossi et al*. [2012].

DEC3 station is mainly affected by two typical meteorological situations. Strong winds arrive at the station predominantly during the winter season with velocities up to 25 m s^{-1} in the direction of the Ebre River (northwest), probably canalized by the watershed. These winds are observed during both daytime and nighttime, and *Barros et al*. [2003] observed a similar pattern. Another typical situation is wind coming from the Mediterranean Sea related to sea breeze episodes, as reported by *Cerralbo et al*. [2015]. Actually, these winds mainly present NW direction during the night and south direction during the day which can indicate changes between land-breeze to sea-breeze atmospheric circulations. They are present during all seasons but are most frequent in summer when the atmospheric mixing in the surface-atmosphere layer leads to a recirculation of the air masses over the flooded and large deltaic area.

The GIC3 high-elevation plateau site is mainly characterized by weak eastern winds coming from the inner Iberian Peninsula with high frequencies and mainly occurring during the nights when they can reach up to 40% of frequency. These low local winds are related to mountain-valley breeze events due to the presence, in the southwest of the station, of the Sierra de Gredos mountain (mean height 2000 m asl). In addition, we also observe northwesterly winds arriving at the station during all the year and with the highest frequency in winter, with speeds between 3 m s^{-1} and 10 m s^{-1}.

3.2.2.2. Regional Influence

In Figure 5 the regional footprints obtained for each station during the period 2012–2015 are presented. The frequency of the passage of simulated back trajectories over each grid cell is shown. During winter, the local influence on the three stations is quite small, atmospheric conditions are real neutral (caused by low insolation and cloudy skies), so air masses tend to come from remote areas due to frontal systems or other synoptic events. As already observed in the windrose plots presented in Figure 4, in winter DEC3 station is mainly reached by strong northwestern winds coming from the north of Spain. This is in agreement with the results observed by other researchers [*Barros et al*., 2003; *Martín et al*., 2011].

In summer, the regional footprints of the stations considerably increase in terms of spatial dimension due to anticyclonic weather conditions. Figure 5 shows that UHU station is reached by air masses that pass over the south of Portugal, while air masses arriving at DEC3 typically originate from the Mediterranean Sea and from the south of the Pyrenees. The air masses arriving at GIC3 station in summer often pass over the south and in the northwest of Spain.

3.2.3. Atmospheric ^{222}Rn Variability

After discussing the seasonal variability of modeled ^{222}Rn fluxes, the dominant local winds, and the regional footprints of each station, we now present an analysis of the diurnal, monthly, and seasonal variability of observed atmospheric ^{222}Rn concentrations together with local ambient temperature and relative humidity.

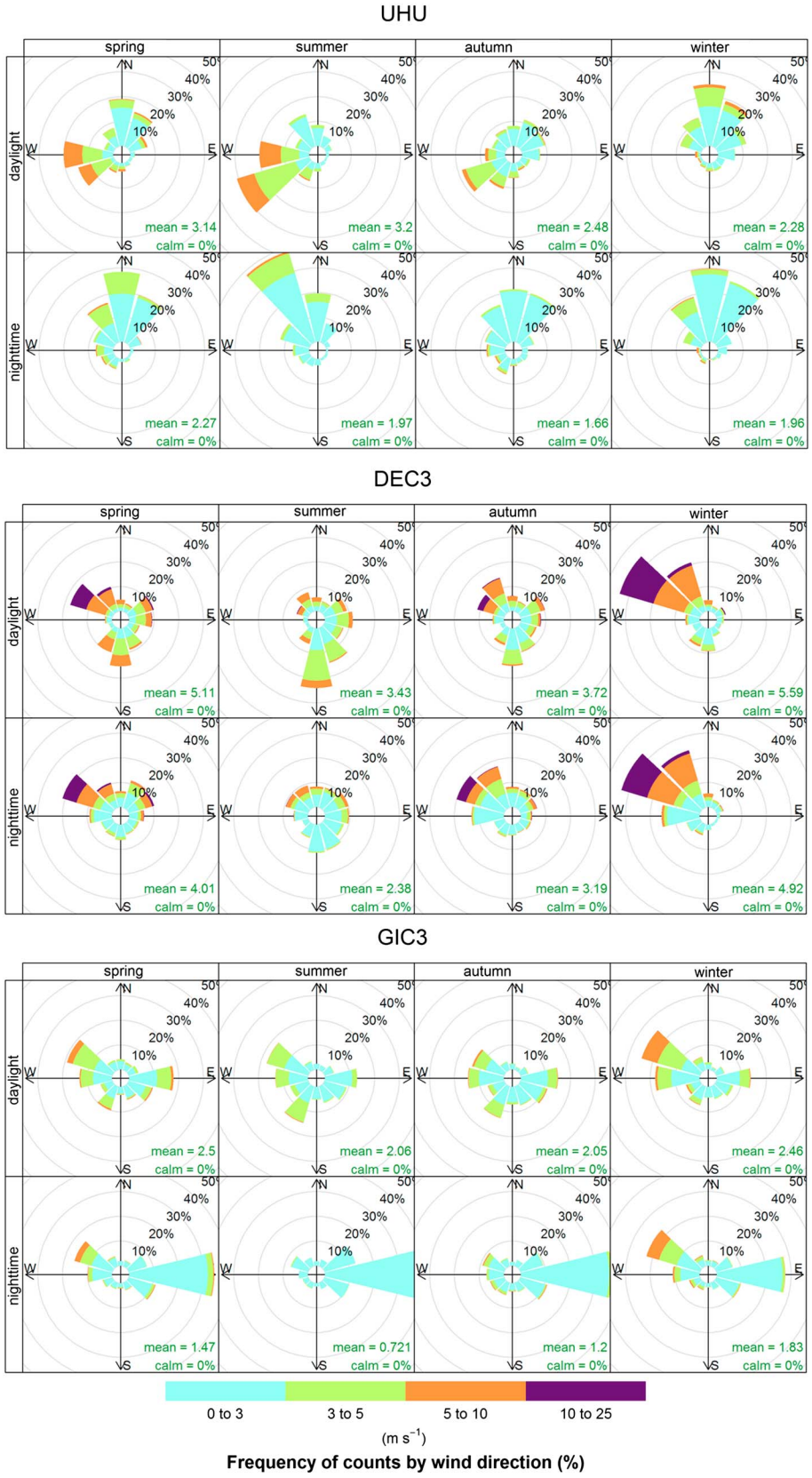

Figure 4. Windrose plots from UHU, DEC3, and GIC3 stations split by seasons and daytime/nighttime.

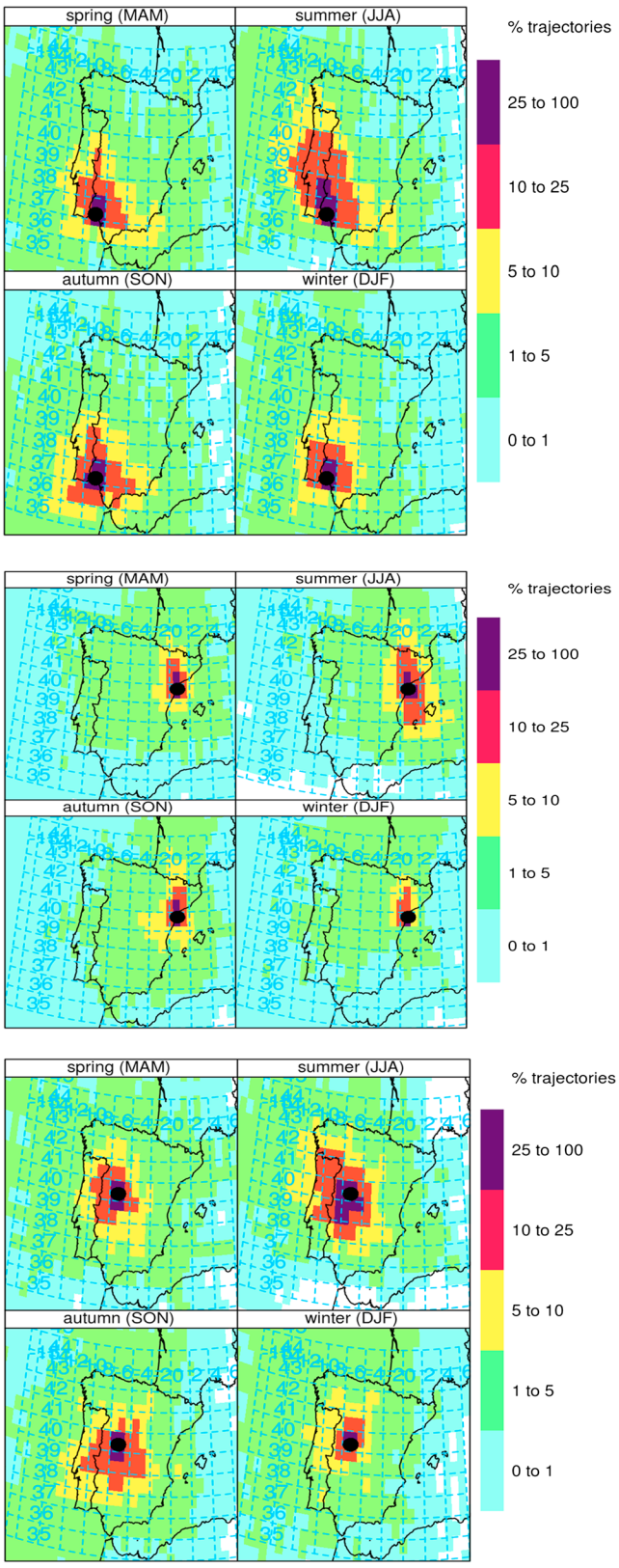

Figure 5. Regional footprints of (top) UHU, (middle) DEC3, and (bottom) GIC3 stations split by season.

Typical and particular seasonal, as well as daily, patterns observed at the stations are highlighted in this section especially.

In Figure 6, 2 years of hourly ^{222}Rn time series are presented at each station. Although the ^{222}Rn concentrations time series is shorter at UHU station, it covers more than 1 year of data and allows investigating the atmospheric variability of ^{222}Rn at a SW site characterized by a low background ^{222}Rn flux source and a potentially high ^{222}Rn flux point source (PG piles) and influenced by Atlantic winds [*Grossi*, 2012; *Hernández-Ceballos et al.*, 2015]. In addition, in Figure 7 composite diurnal patterns of ^{222}Rn, humidity and temperature, split by season are shown for each station with 95% confidence level bands.

The monthly means of atmospheric ^{222}Rn concentrations in Figure 6 show that at GIC3 station, concentrations are characterized by a seasonal cycle with minimum in winter period, when the radon flux is the lowest one (see Table 2), and maximum in summer-autumn period, when highest radon flux has been calculated. Monthly means of ^{222}Rn concentrations at DEC3 and UHU stations do not show any seasonal cycle, but an increase, in the monthly radon means, is observed during autumn-winter seasons. ^{222}Rn concentrations are quite similar at these two stations, except during autumn and winter months, when higher ^{222}Rn concentrations are observed at UHU station than at DEC3 station.

Table S1 in the supporting information gives a summary of the mean ^{222}Rn concentrations measured at each station during each season and over the year with the corresponding 25th, 50th, and 75th percentiles. The amplitude of their diurnal cycle (*A*) is also reported. *A* is calculated as the difference between the maximum and the minimum hourly mean ^{222}Rn concentrations.

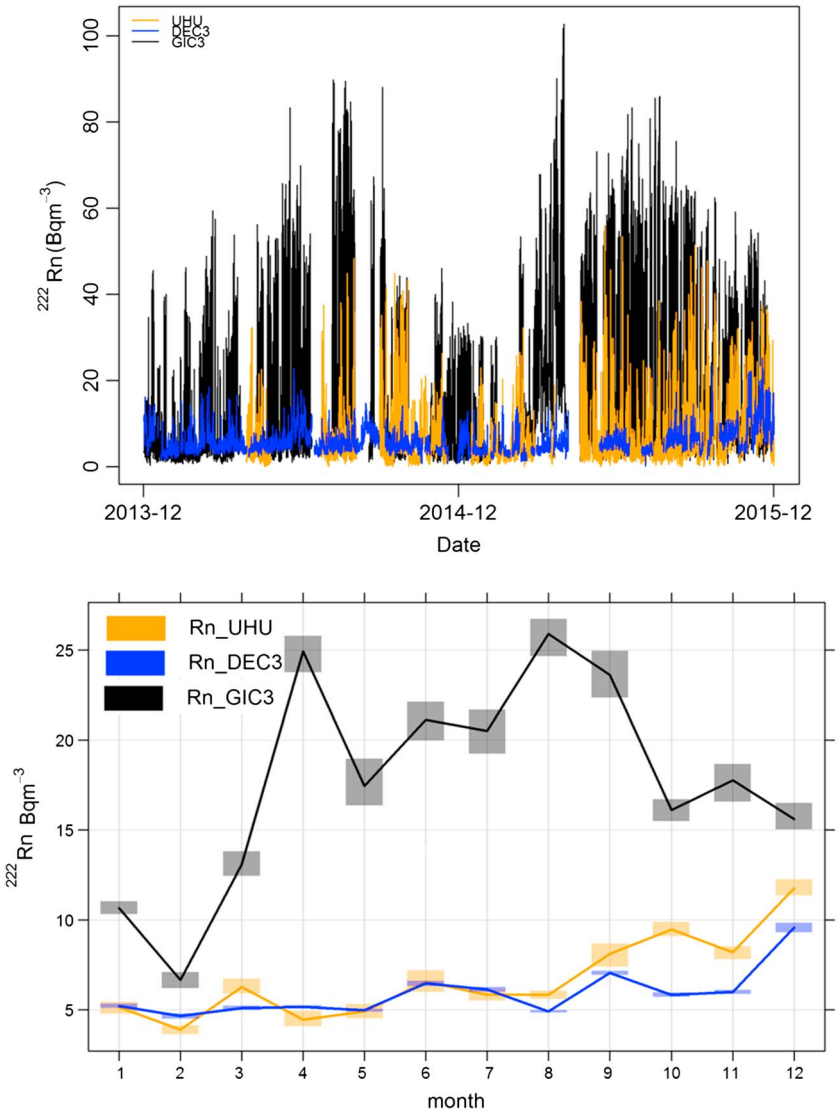

Figure 6. (top) Hourly time series and (bottom) composite monthly variation, with 95% confidence level bands, of atmospheric ^{222}Rn concentrations measured at UHU, DEC3, and GIC3 stations between 2013 and 2015.

At UHU station the highest nocturnal ^{222}Rn concentrations are observed in autumn. This is not in agreement with the modeled ^{222}Rn fluxes, given that a mean value of 26 Bq m$-^{2}$ h^{-1} was obtained for autumn and 36 Bq m$-^{2}$ h^{-1} were calculated for the summer season over the period 2011−2014 (Table 2). In order to understand these results, it is worth noting that Figure 4 indicates a high frequency of calm conditions and weak winds coming from the N-NE in autumn. Under calm nocturnal conditions the planetary boundary layer could be really shallow and this facilitates the accumulation of the exhaled radon from close sources, such as the PG piles located at a distance of approximately 1–2 km from the station.

Measured and estimated ^{222}Rn fluxes from these PG piles range between 50 Bq m^{-2} h^{-1} and 750 Bq m^{-2} h^{-1} depending on soil and atmospheric parameters [*Dueñas et al.*, 2007; *Grossi*, 2012; *López-Coto et al.*, 2014], whereas the radon flux model by *López-Coto et al.* [2013] (basically based on geophysical parameters) only estimated an autumnal ^{222}Rn flux of 26.0 ± 7.8 Bq m^{-2} h^{-1} for the 27 × 27 km^2 grid cell that includes both the UHU station and the PG piles. This means that PG piles, occupying a surface of 1.6% of the total simulated grid cell, could give an additional contribution to the local ^{222}Rn emitted, within the grid cell including the UHU station, between 0.8 Bq m^{-2} h^{-1} and 12 Bq m^{-2} h^{-1}. Under nocturnal conditions the boundary layer height at UHU station can reach quite low values under 20 m agl [*Hernández-Ceballos et al.*, 2015; *Vargas*

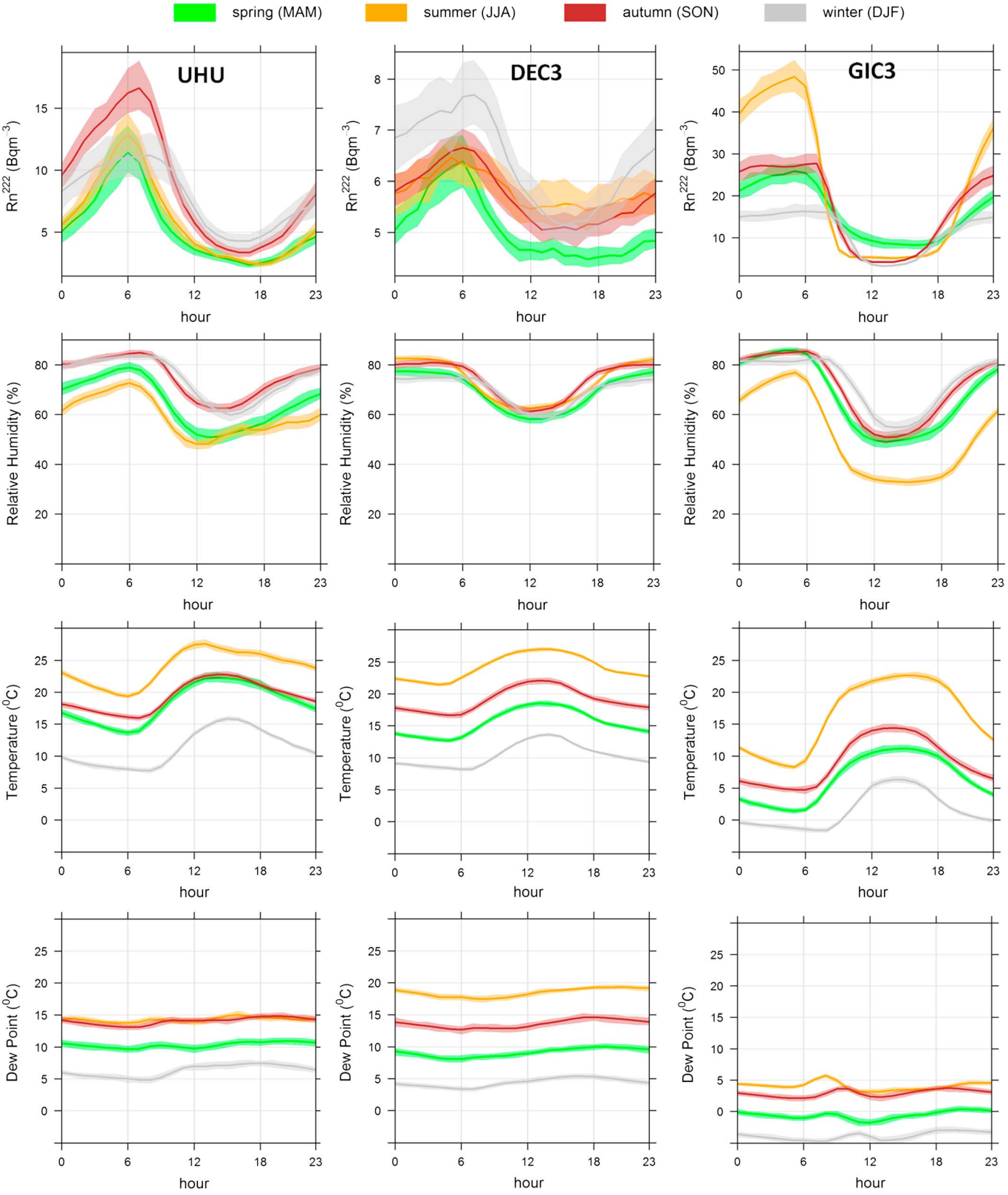

Figure 7. Composite hourly variation of ^{222}Rn concentrations, ambient temperature (°C), and relative humidity (%) measured at each station (left column) UHU, (middle column) DEC3, and (right column) GIC3 split by season. Mean values and 95% confidence intervals are presented.

et al., 2015]; thus, the emitted ^{222}Rn can be accumulated within this layer and significantly increase the measured atmospheric ^{222}Rn concentrations. In winter, the observed shape of the nocturnal increase of the mean atmospheric ^{222}Rn concentration measured at UHU station, after sunset and before sunrise, is quite different to the ones for others seasons. This coincides with the lowest observed temperature (Figure 7) and winds coming from the north in the direction of the mountain with velocities of 3–5 m s^{-1} (Figures 4 and 5). This could be associated with katabatic drainage winds arriving at night at the station from the close mountains and transporting ^{222}Rn to the station.

At DEC3 station winter also presents large variability in ^{222}Rn concentrations and the highest values at night, although modeled ^{222}Rn fluxes are not the highest during this season (Table 2). Comparing Figures 4 and 7, this could probably be explained by the fact that air masses arrive at the station from inland regions transporting ^{222}Rn into the deltaic area. This can also be seen in Figure 5 for the winter footprint. In spring, both ^{222}Rn concentrations and modeled ^{222}Rn fluxes reach a minimum. In this season the DEC3 area is flooded due to the rice production phase and the water will prevent the escape of the ^{222}Rn from the pores of the soil. In addition, the soil of the DEC3 area is mainly constituted by sand which is poor in ^{226}Ra and represents a low radon source [*Grossi et al*., 2012]. Finally, during this season we also observe humid air arriving at the station from the Mediterranean Sea (Figure 7), which can be expected to be poor in ^{222}Rn depending on the time they spent over water bodies before arriving at the station.

Regarding GIC3 station, the high ^{222}Rn flux calculated in summer (about 140 Bq m^{-2} h^{-1}) is due to dry and hot atmospheric conditions that promote radon exhalation from the granitic soil. This, together with the shallow nocturnal boundary layer driven by strong temperature gradients between day and night that takes place in mountain areas, explains the high nocturnal ^{222}Rn concentrations observed at GIC3 station in summer. Summer nocturnal mountain-valley breeze episodes can also guide weak flowing air, rich in radon, to GIC3 from the surrounding granitic mountains. On the contrary, during the day atmospheric ^{222}Rn is diluted into the deeper boundary layer and ^{222}Rn measured at the station decreases due to diurnal mesoscale winds coming from the NW and transporting marine air masses of the Atlantic Ocean (see Figure 5) poor in radon. In agreement with ^{222}Rn flux results, the mean diurnal cycle at the GIC3 station shows the lowest mean ^{222}Rn concentration during the winter at nighttime. This is due to low temperature and frozen soil which drastically reduce ^{222}Rn exhalation from the local sources. In fact, this region is affected by frequent snow episodes in winter. Furthermore, we observed that the nocturnal ^{222}Rn concentrations at GIC3 station, during winter and autumn seasons, show a plateau which could indicate that under stable nocturnal conditions and low atmospheric mixing layer, the height of the nocturnal boundary layer dropped below the 20 m agl measurement height. This last result will be object of further investigations.

4. Conclusions and Outlooks

The objective to expand the existing European network of radon observations and move toward harmonized atmospheric ^{222}Rn data was carried out by the installation of recently improved direct ^{222}Rn monitors (ARMONs) at three contrasting locations in Spain. Atmospheric radon concentrations were monitored at each of the three stations using electrostatic deposition detectors that had been calibrated with a ^{222}Rn chamber as described by *Grossi et al*. [2012]. The response of the ARMON monitor, in uncontrolled environmental conditions, was tested by a comparison study with an established one-filter radon progeny monitor, used at several European stations.

This new high-quality data will provide a much needed enhancement of the European network of ^{222}Rn monitoring stations in the hitherto underrepresented area of southwestern Europe. In the present study a complete analysis of these data, including footprints derived from atmospheric transport models and radon fluxes calculation, has been carried out to understand the main local and regional processes influencing the diurnal and seasonal variability of atmospheric ^{222}Rn concentrations measured at Atlantic (UHU), Mediterranean (DEC3), and high-altitude plateau (GIC3) stations of Spain.

For a short period in summer ARMON detector was compared in parallel with single-filter ^{222}Rn progeny detector at two contrasting locations (coastal DEC3 and mountain KW stations). These comparisons revealed that both monitors are in agreement except for saturated atmospheric conditions or periods of rainfall, when the atmospheric ^{222}Rn concentration measured by the progeny monitor seems to decrease exponentially

with increasing amounts of accumulated rainfall. Unfortunately, the comparison data are not sufficient to derive statistically significant correlations. However, these results represent an important outcome which should be further investigated by a long-lasting comparison study including different atmospheric ^{222}Rn monitors and continuous measurements of aerosol concentrations and meteorological parameters which will help in the harmonization of European radon data.

The results of this study demonstrate the utility of the ARMON detector and its ability to conduct thorough investigations on the variability of F_{eq} of radon progeny and their response to rain intensity, type of rain, and changing aerosol concentrations at different sites. In addition, ARMON could be a reliable ^{222}Rn instrumentation option for high-elevation sites, like Kasprowy Wierch, where atmospheric conditions are often saturated and precipitation surpasses 1 mm for more than half of the year.

^{222}Rn data from DEC3 and UHU stations will be useful to improve mesoscale models of sea-land and ocean-land breeze phenomena, which strongly influence the atmospheric composition and air quality at coastal cities. In the same way, observational data of GIC3 station will help our understanding of mountain-valley breeze phenomena important for the improvement of high-resolution transport models. The significant increase in ^{222}Rn concentrations observed at UHU station under calm conditions confirms results of past studies about the presence of a strong localized artificial radon source close to the station probably associated to phosphogypsum piles (PG). This last result will be analyzed more deeply in our future investigations.

Acknowledgments

Authors want mainly to thank Obra Social "La Caixa" for funding the ClimaDat Project, the Ministerio Español de Economía y Competividad for MIP project (ref. CGL2013-46186-R), and the European commission for the InGOS project (call FP7 Infrastructure project). The research leading to the radon monitors comparison results received funding from a Transnational Access activity offered within the IMECC EU Project (Kasprowy Wierch campaign) and a TTORCH Research Networking Programme Short Visit grant (Delta de l'Ebre campaign). C.G. particularly thanks the Ministerio Español de Educación, Cultura y Deporte, to partially support her work with the research mobility grant "José Castillejos" (ref. CAs15/00042). A.V. thanks the Spanish Ministry of Science for having funded the MATER project (ref. CGL2008-00473/CLI). The work of F.R.V. has been supported by the industrial chair BridGES of the Université de Versailles Saint-Quentin-en-Yvelines, the Commissariat à l' Énergie Atomique et aux Énergies Renouvelables, the Centre National de la Recherche Scientifique, ThalesAleniaSpace, and Veolia S.A. The authors also thank David Carslaw and Karl Ropkins, developers of the R package OpenAir (www.openair-project.org), used in the present work for data analysis. The authors are really grateful to the comments and suggestions of the three reviewers which strongly helped with the improvement of our manuscript. We thank Stefano Galmarini for helping to improve the manuscript. Special thanks are given to the LAO-IC3 team, in the persons of Oscar Batet, Sílvia Borràs, Lídia Cañas, Roger Curcoll Manel Nofuentes, Paola Occhipinti, and Eusebi Vàzquez, for their effort in the maintenance of DEC3 and GIC3 stations. The data set of atmospheric ^{222}Rn concentrations measured at GIC3 and at DEC3 stations is available at www.climadat.es/es/datos/. The data set of UHU station can be directly acquired from je.martin@uhu.es.

References

Baeza, A., et al. (2012), Influence of the Fukushima Dai-ichi nuclear accident on Spanish environmental radioactivity levels, *J. Environ. Rad.*, *114*, 138–145, doi:10.1016/j.jenvrad.2012.03.001.

Barros, N., C. Borrego, I. Toll, C. Soriano, P. Jiménez, and J. M. Baldasano (2003), Urban photochemical pollution in the Iberian Peninsula: Lisbon and Barcelona airsheds, *J. Air Waste Manag. Assoc.*, *53*(3), 347–359, doi:10.1080/10473289.2003.10466157.

Baskaran, M. (2011), Po-210 and Pb-210 as atmospheric tracers and global atmospheric Pb-210 fallout: A review, *J. Environ. Radioact.*, *102*(5), 500–513, doi:10.1016/j.jenvrad.2010.10.007.

Belviso, S., M. Schmidt, C. Yver, M. Ramonet, V. Gros, and T. Launois (2013), Strong similarities between night-time deposition velocities of carbonyl sulphide and molecular hydrogen inferred from semi-continuous atmospheric observations in Gif-sur-Yvette, Paris region, *Tellus B*, *65*, 20719, doi:10.3402/tellusb.v65i0.20719.

Biraud, S., P. Ciais, M. Ramonet, P. Simmonds, V. Kazan, P. Monfray, S. O'Doherty, T. G. Spain, and S. G. Jennings (2000), European greenhouse gas emissions estimated from continuous atmospheric measurements and radon 222 at Mace Head, Ireland, *J. Geophys. Res.*, *105*(D1), 1351–1366, doi:10.1029/1999JD900821.

Bochicchio, F., Z. S. Zunic, C. Carpentieri, S. Antignani, G. Venoso, V. Carelli, C. Cordedda, N. Veselinovic, T. Tollefsen, and P. Bossew (2014), Radon in indoor air of primary schools: A systematic survey to evaluate factors affecting radon concentration levels and their variability, *Indoor Air*, *24*(3), 315–326, doi:10.1111/ina.12073.

Bolívar, J. P. (1995), Aplicaciones de la espectrometría gamma y alfa al estudio del impacto radiactivo producido por industrias no nucleares, PhD thesis. Dept. de Física Atómica, Molecular y Nuclear, Univ. de Sevilla, Sevilla, Spain.

Bolívar, J. P., R. García-Tenorio, and M. García-León (1996), Radioactive impact of some phosphogypsum piles in soils and salt marshes evaluated by γ-ray spectrometry, *Appl. Radiat. Isot.*, *47*(9–10), 1969–1075, doi:10.1016/S0969-8043(96)00108-X.

Bolívar, J. P., R. García-Tenorio, J. L. Mas, and F. Vaca (2002), Radioactive impact in sediments from an estuarine system affected by industrial wastes releases, *Environ. Int.*, *27*(8), 639–645, doi:10.1016/S0160-4120(01)00123-4.

Bossew, P., et al. (2014), Geographical distribution of the annual mean radon concentrations in primary schools of Southern Serbia—Application of geostatistical methods, *J. Environ. Radioact.*, *127*, 141–148, doi:10.1016/j.jenvrad.2013.09.015.

Cerralbo, P., M. Grifoll, J. Moré, M. Bravo, A. Sairouní Afif, and M. Espino (2015), Wind variability in a coastal area (Alfacs Bay, Ebro River delta), *Adv. Sci. Res.*, *12*, 11–21, doi:10.5194/asr-12-11-2015.

Chambers, S. D., A. G. Williams, W. Zahorowski, A. Griffiths, and J. Crawford (2011), Separating remote fetch and local mixing influences on vertical radon measurements in the lower atmosphere, *Tellus B*, *63*(5), 843–859, doi:10.1111/j.1600-0889.2011.00565.x.

Chambers, S. D., W. Zahorowski, A. G. Williams, J. Crawford, and A. D. Griffiths (2013), Identifying tropospheric baseline air masses at Mauna Loa Observatory between 2004 and 2010 using Radon-222 and back trajectories, *J. Geophys. Res. Atmos.*, *118*, 992–1004, doi:10.1029/2012JD018212.

Chambers, S. D., S. B. Hong, A. G. Williams, J. Crawford, A. D. Griffiths, and S. J. Park (2014), Characterising terrestrial influences on Antarctic air masses using Radon-222 measurements at King George Island, *Atmos. Chem. Phys.*, *14*, 9903–9916, doi:10.5194/acp-14-9903-2014.

Chambers, S. D., et al. (2015), Towards a universal "baseline" characterisation of air masses for high- and low-altitude observing stations using Radon-222, *Aerosol Air Qual. Res.*, *16*, 885–899, doi:10.4209/aaqr.2015.06.0391.

Chambers, S. D., D. Galeriu, A. G. Williams, A. Melintescu, A. D. Griffiths, J. Crawford, L. Dyer, M. Duma, and B. Zorila (2016), Atmospheric stability effects on potential radiological releases at a nuclear research facility in Romania: Characterising the atmospheric mixing state, *J. Environ. Radioact.*, *154*, 68–82, doi:10.1016/j.jenvrad.2016.01.010.

Chevillard, A., et al. (2002), Transport of ^{222}Rn using the regional model REMO: A detailed comparison with measurements over Europe, *Tellus B*, *54*(5), 850–871, doi:10.1034/j.1600-0889.2002.01339.x.

Chmura, L., K. Rozanski, J. M. Necki, M. Zimnoch, A. Korus, and M. Pycia (2008), Atmospheric concentrations of carbon dioxide in Southern Poland: Comparison of mountain and urban environments, *Pol. J. Environ. Stud.*, *17*(6), 859–867.

De Martino, S., and C. Sabbarese (1997), A method for emanation coefficient measurements of ^{222}Rn and ^{220}Rn from soils, *Phys. Chem. Earth*, *22*(1–2), 19–23, doi:10.1016/S0079-1946(97)00072-4.

Draxler, R. R., and G. D. Hess (1998), An overview of the HYSPLIT_4 modelling system for trajectories, dispersion, and deposition, *Aust. Meteor. Mag.*, *47*, 295–308.

Dueñas, C., E. Liger, S. Cañete, M. Pérez, and J. P. Bolívar (2007), Exhalation of ^{222}Rn from phosphogypsum piles located at the Southwest of Spain, *J. Environ. Radioact.*, *95*(2–3), 63–74, doi:10.1016/j.jenvrad.2007.01.012.

Fleischer, R. L., W. R. Giard, A. Mogro-Campero, L. G. Turner, H. W. Alter, and J. E. Gingrich (1980), Dosimetry of environmental radon: Methods and theory of low-dose, integrated measurements, *Health Phys.*, *39*, 957–62, doi:10.1097/00004032-198012000-00009.

Fujinami, N. (1996), Observational study of the scavenging of radon daughters by precipitation from the atmosphere, *Environ. Int.*, *22*(S1), 181–185, doi:10.1016/S0160-4120(96)00106-7.

Galmarini, S. (2006), One year of ^{222}Rn concentration in the atmospheric surface layer, *Atmos. Chem. Phys.*, *6*, 2865–2887, doi:10.5194/acp-6-2865-2006.

Gangoiti, G., L. Alonso, M. Navazo, A. Albizuri, G. Perez-Landa, M. Matabuena, V. Valdenebro, M. Maruri, J. A. García, and M. M. Millán (2002), Regional transport of pollutants over the Bay of Biscay: Analysis of an ozone episode under a blocking anticyclone in west-central Europe, *Atmos. Environ.*, *36*(8), 1349–1361, doi:10.1016/S1352-2310(01)00536-2.

García, M. A., A. Sánchez-Arcilla, J. P. Sierra, J. Sospedra, and J. Gómez (1993), Wind waves off the Ebro Delta, NW Mediterranean, *J. Mar. Syst.*, *4*(2–3), 235–262, doi:10.1016/0924-7963(93)90012-B.

Griffiths, A. D., W. Zahorowski, A. Element, and S. Werczynski (2010), A map of radon flux at the Australian land surface, *Atmos. Chem. Phys.*, *10*, 8969–8982, doi:10.5194/acp-10-8969-2010.

Grossi, C., A. Vargas, A. Camacho, I. López-Coto, J. P. Bolívar, X. Yu, and F. Conen (2011), Inter-comparison of different direct and indirect methods to determine radon flux from soil, *Radiat. Meas.*, *46*(1), 112–118, doi:10.1016/j.radmeas.2010.07.021.

Grossi, C. (2012), ^{222}Rn as tracer for air mass transport Characterization at a 100-m-high tower on the Southwest Spanish coast, PhD thesis, Institut de Tècniques Energètiques, Univ. Politècnica de Catalunya, Barcelona, Spain.

Grossi, C., D. Arnold, J. A. Adame, I. López-Coto, J. P. Bolívar, B. A. de la Morena, and A. Vargas (2012), Atmospheric ^{222}Rn concentration and source term at *El Arenosillo* 100 m meteorological tower in southwest Spain, *Radiat. Meas.*, *47*(2), 149–162, doi:10.1016/j.radmeas.2011.11.006.

Grossi, C., F. R. Vogel, J. A. Morguí, R. Curcoll, A. Àgueda, O. Batet, M. Nofuentes, P. Occhipinti, A. Vargas, and X. Rodó (2014), First estimation of CH_4 fluxes using the ^{222}Rn tracer method over the central Iberian Peninsula, in *Air Pollution XXII, WIT Transactions on Ecology and the Environment*, vol. 183, pp. 233–245, WIT Press, Southampton, U. K., doi:10.2495/AIR140201.

Hatakka, J., et al. (2003), Overview of the atmospheric research activities and results at Pallas GAW station, *Boreal Environ. Res.*, *8*(4), 365–383.

Hernández-Ceballos, M. A., J. A. Adame, J. P. Bolívar, and B. A. De la Morena (2013), Vertical behaviour and meteorological properties of air masses in the southwest of the Iberian Peninsula (1997–2007), *Meteorol. Atmos. Phys.*, *119*(3), 163–175, doi:10.1007/s00703-012-0225-5.

Hernández-Ceballos, M. A., A. Vargas, D. Arnold, and J. P. Bolívar (2015), The role of mesoscale meteorology in modulating the ^{222}Rn concentrations in Huelva (Spain)—Impact of phosphogypsum piles, *J. Environ. Radioact.*, *145*, 1–9, doi:10.1016/j.jenvrad.2015.03.023.

Hirao, S., H. Yamazawa, and J. Moriizumi (2010), Inverse modelling of Asian ^{222}Rn flux using surface air ^{222}Rn concentration, *J. Environ. Radioact.*, *101*(11), 974–984, doi:10.1016/j.jenvrad.2010.07.004.

Horng, M. C., and S. H. Jiang (2004), In situ measurements of gamma-ray intensity from radon progeny in rainwater, *Radiat. Meas.*, *38*(1), 23–30, doi:10.1016/S1350-4487(03)00285-3.

International Atomic Energy Agency (2012), Sources and measurements of radon and radon progeny applied to climate and air quality studies. Proceedings of a technical meeting held in Vienna, organized by the International Atomic Energy Agency and cosponsored by the World Meteorological Organization, IAEA, Vienna.

Izquierdo, R., M. Alarcón, L. Aguillaume, and A. Àvila (2014), Effects of teleconnection patterns on the atmospheric routes, precipitation and deposition amounts in the north-eastern Iberian Peninsula, *Atmos. Environ.*, *89*, 482–490, doi:10.1016/j.atmosenv.2014.02.057.

Jagielski, J., H. Viguier, J. P. Frontier, P. Trouslard, B. Kopcewicz, M. Kopcewicz, and L. Thomé (1996), PIXE study of atmospheric aerosols in mountain region of Poland, *Nucl. Instrum. Methods Phys. Res., Sect. B*, *118*(1–4), 388–391, doi:10.1016/0168-583X(95)01085-8.

Jorba, O., C. Pérez, F. Rocadenbosch, and J. M. Baldasano (2004), Cluster analysis of 4-day back trajectories arriving in the Barcelona area, Spain, from 1997 to 2002, *J. Appl. Meteorol.*, *43*, 887–901, doi:10.1175/1520-0450(2004)043<0887:CAODBT>2.0.CO;2.

Kamra, L. (2015), Seasonal emanation of radon at Ghuttu, northwest Himalaya: Differentiation of atmospheric temperature and pressure influences, *Appl. Radiat. Isot.*, *105*, 170–175, doi:10.1016/j.apradiso.2015.08.031.

Karstens, U., C. Schwingshackl, D. Schmithüsen, and I. Levin (2015), A process-based ^{222}radon flux map for Europe and its comparison to long-term observations, *Atmos. Chem. Phys.*, *15*, 12,845–12,865, doi:10.5194/acp-15-12845-2015.

Levin, I., H. Glatzel-Mattheier, T. Marik, M. Cuntz, M. Schmidt, and D. E. J. Worthy (1999), Verification of German methane emission inventories and their recent changes based on atmospheric observations, *J. Geophys. Res.*, *104*(D3), 3447–3456, doi:10.1029/1998JD100064.

Levin, I., M. Born, M. Cuntz, U. Langendörfer, S. Mantsch, T. Naegler, M. Schmidt, A. Varlagin, S. Verclas, and D. Wagenbach (2002), Observations of atmospheric variability and soil exhalation rate of radon-222 at a Russian forest site. Technical approach and deployment for boundary layer studies, *Tellus B*, *54*(5), 462–475, doi:10.1034/j.1600-0889.2002.01346.x.

Levin, I., D. Schmithüsen, and A. Vermeulen (2016), Assessment of 222 radon progeny loss in long tubing based on static filter measurements in the laboratory and in the field, *Atmos. Meas. Tech. Discuss.*, doi:10.5194/amt-2016-112, in review, 2016.

Locatelli, R., et al. (2015), Atmospheric transport and chemistry of trace gases in LMDz5B: Evaluation and implications for inverse modelling, *Geosci. Model Dev.*, *8*, 129–150, doi:10.5194/gmd-8-129-2015.

López-Coto, I., J. L. Mas, and J. P. Bolívar (2013), A 40-year retrospective European radon flux inventory including climatological variability, *Atmos. Environ.*, *73*, 22–33, doi:10.1016/j.atmosenv.2013.02.043.

López-Coto, I., J. L. Mas, A. Vargas, and J. P. Bolívar (2014), Studying radon exhalation rates variability from phosphogypsum piles in the SW of Spain, *J. Hazard. Mater.*, *280*, 464–471, doi:10.1016/j.jhazmat.2014.07.025.

Łupikasza, E. (2010), Spatial and temporal variability of extreme precipitation in Poland in the period 1951–2006, *Int. J. Climatol.*, *30*(7), 991–1007, doi:10.1002/joc.1950.

Martín, M., J. Plaza, M. D. Andrés, J. C. Bezares, and M. M. Millán (1991), Comparative study of seasonal air pollutant behaviour in a Mediterranean coastal site: Castellon (Spain), *Atmos. Environ.*, *25*(8), 1523–1535, doi:10.1016/0960-1686(91)90012-V.

Martín, M. L., F. Valero, A. Pascual, A. Morata, and M. Y. Luna (2011), Springtime connections between the large-scale sea-level pressure field and gust wind speed over Iberia and the Balearics, *Nat. Hazards Earth Syst. Sci.*, *11*, 191–203, doi:10.5194/nhess-11-191-2011.

Morawska, L. (1989), Two ways of determining the ^{222}Rn emanation coefficient, *Health Phys.*, *57*(3), 481–483.

Nazaroff, W. W. (1992), Radon transport from soil to air, *Rev. Geophys.*, *30*(2), 137–160, doi:10.1029/92RG00055.

Nazaroff, W. W. (2013), Exploring the consequences of climate change for indoor air quality, *Environ. Res. Lett.*, *8*(1), 15,022–15,042, doi:10.1088/1748-9326/8/1/015022.

Nazaroff, W. W., and A. V. Nero (Eds) (1988), *Radon and Its Decay Products in Indoor Air*, John Wiley, New York.
Niedźwiedź, T., E. Łupikasza, I. Pińskwar, Z. W. Kundzewicz, M. Stoffel, and L. Małarzewski (2014), Variability of high rainfalls and related synoptic situations causing heavy floods at the northern foothills of the Tatra Mountains, *Theor. Appl. Climatol.*, *119*(1), 273–284, doi:10.1007/s00704-014-1108-0.
Pitari, G., E. Coppari, N. De Luca, and P. Di Carlo (2014), Observations and box model analysis of radon-222 in the atmospheric surface layer at L'Aquila, Italy: March 2009 case study, *Environ Earth Sci.*, *71*, 2353, doi:10.1007/s12665-013-2635-1.
Porstendorfer, J. (1994), Properties and behaviour of radon and thoron and their decay products in the air, *J. Aerosol Sci.*, *25*(2), 219–263, doi:10.1016/0021-8502(94)90077-9.
Porstendorfer, J., C. Zock, and A. Reineking (2000), Aerosol size distribution of the radon progeny in outdoor air, *J. Environ. Rad.*, *51*(1), 37–48, doi:10.1016/s0265-931x(00)00043-6.
Spurny, K. R. (Ed) (1999), *Analytical Chemistry of Aerosols: Science and Technology*, CRC Press LLC, Florida.
Stein, A. F., R. R. Draxler, G. D. Rolph, B. J. B. Stunder, M. D. Cohen, and F. Ngan (2015), NOAA's HYSPLIT atmospheric transport and dispersion modeling system, *Bull. Am. Meteorol. Soc.*, *96*, 2059–2077, doi:10.1175/BAMS-D-14-00110.1.
Szegvary, T., F. Conen, and P. Ciais (2009), European ^{222}Rn inventory for applied atmospheric studies, *Atmos. Environ.*, *43*(8), 1536–1539, doi:10.1016/j.atmosenv.2008.11.025.
Rafique, M., S. U. Rahman, T. Mahmood, S. Rahman, Matiullah, and S. U. Rehman (2011), Radon exhalation rate from soil, sand, bricks, and sedimentary samples collected from Azad Kashmir, Pakistan, *Russ. Geol. Geophys.*, *52*(4), 450–457, doi:10.1016/j.rgg.2011.03.007.
Taguchi, S., R. M. Law, C. Rödenbeck, P. K. Patra, S. Maksyutov, W. Zahorowski, H. Sartorius, and I. Levin (2011), TransCom continuous experiment: Comparison of ^{222}Rn transport at hourly time scales at three stations in Germany, *Atmos. Chem. Phys.*, *11*, 10,071–10,084, doi:10.5194/acp-11-10071-2011.
Tanner, A. B. (1980), Radon migration in the ground: A supplementary review, in *The Natural Radiation Environment I11*, *CONF 780422*, edited by T. F. Gesell and W. M. Lowder, pp. 5–56, U.S. Department of Energy, Washington, D. C.
Vargas, A., X. Ortega, and J. L. Martín Matarranz (2004), Traceability of radon-222 activity concentration in the radon chamber at the technical university of Catalonia (Spain), *Nucl. Instrum. Methods Phys. Res., Sect. A*, *526*(3), 501–509, doi:10.1016/j.nima.2004.02.022.
Vargas, A., and X. Ortega (2006), Influence of environmental changes on continuous radon monitors. Results of a Spanish intercomparison exercise, *Radiat. Prot. Dosimetry*, *121*(3), 303–309, doi:10.1093/rpd/ncl036.
Vargas, A., D. Arnold, J. A. Adame, C. Grossi, M. A. Hernández-Ceballos, and J. P. Bolívar (2015), Analysis of the vertical radon structure at the Spanish "El Arenosillo" tower station, *J. Environ. Radioact.*, *139*, 1–17, doi:10.1016/j.jenvrad.2014.09.018.
Vinuesa, J. F., S. Basu, and S. Galmarini (2007), The diurnal evolution of ^{222}Rn and its progeny in the atmospheric boundary layer during the Wangara experiment, *Atmos. Chem. Phys.*, *7*, 5003–5019, doi:10.5194/acp-7-5003-2007.
Vogel, F. R., M. Ishizawa, E. Chan, D. Chan, S. Hammer, I. Levin, and D. E. J. Worthy (2012), Regional non-CO_2 greenhouse gas fluxes inferred from atmospheric measurements in Ontario, Canada, *J. Integr. Environ. Sci.*, *9*(S1), 1–15, doi:10.1080/1943815X.2012.691884.
Vogel, F. R., B. Tiruchittampalam, J. Theloke, R. Kretschmer, C. Gerbig, S. Hammer, and I. Levin (2013), Can we evaluate a fine-grained emission model using high-resolution atmospheric transport modelling and regional fossil fuel CO_2 observations?, *Tellus B*, *65*, 18681, doi:10.3402/tellusb.v65i0.18681.
Wada, A., H. Matsueda, S. Murayama, S. Taguchi, S. Hirao, H. Yamazawa, J. Moriizumi, K. Tsuboi, Y. Niwa, and Y. Sawa (2013), Quantification of emission estimates of CO_2, CH_4 and CO for East Asia derived from atmospheric radon-222 measurements over the western North Pacific, *Tellus B*, *65*, 18037, doi:10.3402/tellusb.v65i0.18037.
Weller, R., I. Levin, D. Schmithüsen, M. Nachbar, J. Asseng, and D. Wagenbach (2014), On the variability of atmospheric ^{222}Rn activity concentrations measured at Neumayer, coastal Antarctica, *Atmos. Chem. Phys.*, *14*, 3843–3853, doi:10.5194/acp-14-3843-2014.
Whittlestone, S., and W. Zahorowski (1998), Baseline radon detectors for shipboard use: Development and deployment in the First Aerosol Characterization Experiment (ACE 1), *J. Geophys. Res.*, *103*(D13), 16,743–16,751, doi:10.1029/98JD00687.
Williams, A. G., W. Zahorowski, S. Chambers, A. Griffiths, J. M. Hacker, A. Element, and S. Werczynski (2011), The vertical distribution of radon in clear and cloudy daytime terrestrial boundary layers, *J. Atmos. Sci.*, *68*(1), 155–174, doi:10.1175/2010JAS3576.1.
Williams, A. G., S. Chambers, and A. Griffiths (2013), Bulk mixing and decoupling of the nocturnal stable boundary layer characterized using a ubiquitous natural tracer, *Boundary Layer Meteorol.*, *149*(3), 381–402, doi:10.1007/s10546-013-9849-3.
Xia, Y., H. Sartorius, C. Schlosser, U. Stöhlker, F. Conen, and W. Zahorowski (2010), Comparison of one- and two-filter detectors for atmospheric ^{222}Rn measurements under various meteorological conditions, *Atmos. Meas. Tech.*, *3*, 723–731, doi:10.5194/amt-3-723-2010.
Zahorowski, W., S. D. Chambers, and A. Henderson-Sellers (2004), Ground based radon-222 observations and their application to atmospheric studies, *J. Environ. Radioact.*, *76*(1–2), 3–33, doi:10.1016/j.jenvrad.2004.03.033.
Zahorowski, W., S. D. Chambers, T. Wang, C.-H. Kang, I. Uno, S. Poon, S.-N. Oh, S. Wcrczynski, J. Kim, and A. Henderson-Sellers (2005), Radon-222 in boundary layer and free tropospheric continental outflow events at three ACE-Asia sites, *Tellus B*, *57*, 124–140, doi:10.3402/tellusb.v57i2.16776.
Zimnoch, M., P. Wach, L. Chmura, Z. Gorczyca, K. Rozanski, J. Godlowska, J. Mazur, K. Kozak, and A. Jericevic (2014), Factors controlling temporal variability of near-ground atmospheric ^{222}Rn concentration over central Europe, *Atmos. Chem. Phys.*, *14*, 9567–9581, doi:10.5194/acp-14-9567-2014.